



JP0150533

JAERI-Conf 2001-002

ICANS-XV

15th Meeting of the International Collaboration on Advanced
Neutron Sources
November 6-9, 2000
Tsukuba, Japan

9.3

Quasielastic High-Resolution Time-of-Flight Spectrometers Employing Multi-Disk Chopper Cascades for Spallation Sources

R. E. Lechner

Hahn-Meitner-Institut, Abt. SF1 / BENSC, Glienicker Straße 100, D-14109 Berlin, Germany
E-mail: lechner@hmi.de

Abstract

The design of multi-disk chopper time-of-flight (MTOF) spectrometers for high-resolution quasielastic and low-energy inelastic neutron scattering at spallation sources is discussed in some detail. A continuously variable energy resolution (1 μ eV to 10 meV), and a large dynamic range (1 μ eV to 100 meV), are outstanding features of this type of instrument, which are easily achieved also at a pulsed source using state-of-the-art technology.

The method of intensity-resolution optimization of MTOF spectrometers at spallation sources is treated on the basis of the requirement of using (almost) 'all the neutrons of the pulse', taking into account the constant, but wavelength-dependent duration of the source pulse. It follows, that the optimization procedure (which is slightly different from that employed in the steady-state source case) should give priority to the highest resolution, whenever such a choice becomes necessary. This leads to long monochromator distances (L_{12}) of the order of 50 m, for achieving resolutions now available at reactor sources. A few examples of spectrometer layout and corresponding design parameters for large-angle and for small-angle quasielastic scattering instruments are given. In the latter case higher energy resolution than for large-angle scattering is required and achieved. The use of phase-space transformers, neutron wavelength band-pass filters and multichromatic operation for the purpose of intensity-resolution optimization are discussed.

This spectrometer can be designed to make full use of the pulsed source peak flux. Therefore, and because of a number of improvements, high resolution will be available at high intensity: for any given resolution the total intensity at the detectors, when placed at one of the planned new spallation sources (SNS, JSNS, ESS, AUSTRON) will be larger by at least three orders of magnitude than the total intensity of any of the presently existing instruments of this type in routine operation at steady-state sources.

1. Introduction

Atomic and molecular motions accessible to neutron scattering studies generally cover many orders of magnitude in space and time. Therefore they require measurement techniques employing an extensive range of resolutions. While other instruments competing in the same fields usually provide only a few discrete values of (e.g. the elastic) energy resolution, one of the essential advantages of multi-disk chopper time-of-flight (MTOF) spectrometers is the fact, that their energy resolution can be varied continuously over a large range. This has been

demonstrated during many years of successful experiments with the existing spectrometers of this type (see below). In recent work [1,2] the characteristics of a proposed quasielastic high-resolution MTOF spectrometer for spallation sources was described. The concept of this new instrument is derived from the three MTOF spectrometers in successful operation at continuous neutron sources, IN5 (at ILL in Grenoble) [3-5], MIBEMOL (at LLB in Saclay) [6] and NEAT (at BENSC in Berlin) [7], the latter being at present the most advanced instrument of this kind. The performance with respect to energy resolution was chosen to be similar, but slightly improved, as compared to that of NEAT. Since there is no „bad“ resolution, it is important to extend previously available resolution ranges not only beyond the upper limit, but beyond the lower limit as well. The “standard” energy resolution of the proposed instrument is continuously variable over 4 orders of magnitude in the range from 1 μeV to 10 meV. Optimization with respect to intensity at given resolution obviously requires an adaptation of the spectrometer design parameters properly taking into account the time structure of the pulsed source. The main object of the proposal was to show, that after this adaptation – because of an improved design and due to fully exploiting the pulsed source peak flux – an enormous gain in total intensity at the detectors (by three orders of magnitude, if the instrument is placed at the AUSTRON source) is achieved for any given energy resolution, as compared to the above-mentioned existing instruments. In the present paper essential details of intensity and resolution (Sec. 2) and of the optimization method (Sec. 3) are first discussed in general terms. Then the application of this method to MTOF instruments at pulsed sources will be considered (Sec. 4) and several versions of such spectrometers for the case of large-angle quasielastic neutron scattering and for quasielastic small-angle scattering will be described. A number of beam-optical and time-dependent filtering tools available for this purpose are discussed (Sec. 5). Finally total intensity gain factors are given (Sec. 6).

2. MTOF spectrometers : Intensity and Resolution

In the following the “instrument intensity” will be defined as the total number of neutrons, which after having been scattered by a standard sample (e. g. a vanadium plate scattering 10 % of the incident beam), are counted per unit of time, integrated over all detectors of the spectrometer. At specified resolution, the three existing MTOF-instruments, IN5, MIBEMOL and NEAT, all located at steady-state reactors, have approximately equal intensities, inspite of the large differences in the power of the respective sources. This is a consequence of the fact, that the efficiency of these spectrometers increases in the above order, due to specific improvements of the design [7,8]. As usual, in order to make further progress, we expect future spectrometers to benefit from the best ideas available at the time. Below, I will outline, what I consider to be the basic principles and the state-of-the-art tools to be used in the layout of the next MTOF spectrometer generation.

We start with the basic formulae for intensity and resolution [9,10]. The definitions of those distances and chopper opening times (pulse widths) that are relevant for the calculation of these quantities are defined in the schematic drawing of Fig. 1. It shows two disk choppers, CH1 and CH2, at a distance L_{12} from each-other, serving as the pulsed monochromator. The neutron beam incident on CH1 is chopped into “white” pulses with width in time (FWHM) τ_1 , whereas CH2 creates narrow-bandwidth “monochromatic” pulses (mean wavelength λ_0) with time width τ_2 . A set of additional filter disk-choppers is placed in between, to prevent neutrons with wavelengths outside of the selected band from simultaneously arriving at CH2 (primary overlap : removal of different-order contamination) and to avoid the simultaneous arrival at the detectors of scattered neutrons originating from different pulses (secondary

overlap : frame overlap prevention). The sample is placed at a distance L_{2S} from CH2, and the detectors are at a distance L_{SD} from the sample.

The total intensity at the detectors is given by :

$$I = c \cdot \Phi(\lambda_0) \cdot T_g(\lambda_0) \cdot [(\tau_1 \cdot \tau_2) / (L_{12} P)] \cdot \int d\Omega \quad (1)$$

where $\Phi(\lambda_0)$ is the incident differential neutron flux at the wavelength λ_0 , per unit of wavelength, arriving at the first chopper, integrated over the beam divergence allowed for by the guide. $T_g(\lambda_0)$ is the (wavelength-dependent) transmission of the guide delivering the neutron beam from the moderator to the sample, and $\int d\Omega$ is the total solid angle covered by the detectors of the instrument. The constant c in front of the expression contains the required physical constants; it may also include adjustment factors for small corrections, as well as a constant factor depending on the units and on the definition of the opening times used. (For instance one may want to employ the standard deviation or other parameters characterizing the chopper burst time distributions, rather than the FWHM). Obviously, at a continuous source, the intensity is proportional to the inverse time-of-flight period P . It can be chosen within certain practical limits and is set according to the desired length of the spectrum P_{spec} , which is (typically) given by

$$P [\mu s] = 1.5 \cdot \lambda_0 [\text{\AA}] \cdot L_{SD} [\text{m}] \cdot 252.78 = P_{spec} \quad (2)$$

If L_{SD} is fixed (e.g. for budgetary reasons, in a large-angle spectrometer), it is seen, that the intensity (eq. (1)) is controlled by a factor determined by the design of the chopper cascade, $F_i = (\tau_1 \cdot \tau_2) / L_{12}$. Once all the spectrometer distances are fixed, which is in general likely to be the case, except for selected (e.g. small) angles, where L_{SD} may be a variable, relations (1) and (2) show, that the intensity for given incident neutron wavelength is essentially governed by the factor $(\tau_1 \cdot \tau_2)$, i.e. the product of the two chopper opening times. The latter also control the resolution, and we will see immediately, how intensity and resolution are connected through these parameters.

The energy resolution width (FWHM) at the detector [9,10], i.e. the uncertainty in the experimentally determined energy transfer $h\nu$, is given by

$$\Delta(h\nu) [\mu\text{eV}] = 647.2 (A^2 + B^2 + C^2)^{1/2} / (L_{12} \cdot L_{SD} \cdot \lambda^3) \quad (3)$$

$$A = 252.78 \cdot \Delta L \cdot \lambda \cdot L_{12} \quad (3a)$$

$$B = \tau_1 (L_{2S} + L_{SD} \cdot \lambda^3 / \lambda_0^3) \quad (3b)$$

$$C = \tau_2 (L_{12} + L_{2S} + L_{SD} \cdot \lambda^3 / \lambda_0^3) \quad (3c)$$

where ΔL is the uncertainty in the length of the neutron flight path, depending mainly on beam divergence, sample geometry and detector thickness. We note that the energy dependent resolution strongly depends on the scattered neutron wavelength λ , whereas the total intensity, as an integral property of the spectrometer, has no such dependence. From eqs. (1) to (3) the following is evident : i) High resolution is favoured by short pulse widths and large values of L_{12} and L_{SD} . ii) If the distances are fixed (as is the case of a given spectrometer or spectrometer configuration) and if sample geometry, incident wavelength and energy transfer have been chosen, then the total-intensity and resolution-width functions can only be varied

by changing the chopper opening times τ_1 and τ_2 . iii) It is also clear, that both functions decrease, when the chopper pulse widths are reduced.

3. Pulse-Width Ratio (PWR) optimization

In order to achieve best instrument performance, one must not only consider the two pulse widths, τ_1 and τ_2 , individually, but especially also their ratio, which is a rather important parameter. The question, how to optimize the pulse-width ratio $\rho = \tau_1 / \tau_2$ has been treated previously [10] and further discussed [11] in the context of the conception of the spectrometer NEAT. The answer is, that the intensity I is maximized for a given value of the resolution $\Delta(hv)$, and equivalently, the resolution width $\Delta(hv)$ is minimized for a given intensity I , under the following condition for the optimum of the ratio ρ of the two chopper opening times:

$$\rho_{\text{opt}} = (L_{12} + L_{2S} + L_{SD} \cdot \lambda^3 / \lambda_0^3) / (L_{2S} + L_{SD} \cdot \lambda^3 / \lambda_0^3) \quad (4)$$

which is equivalent with the requirement, that the terms B and C in eq. (3) should be made

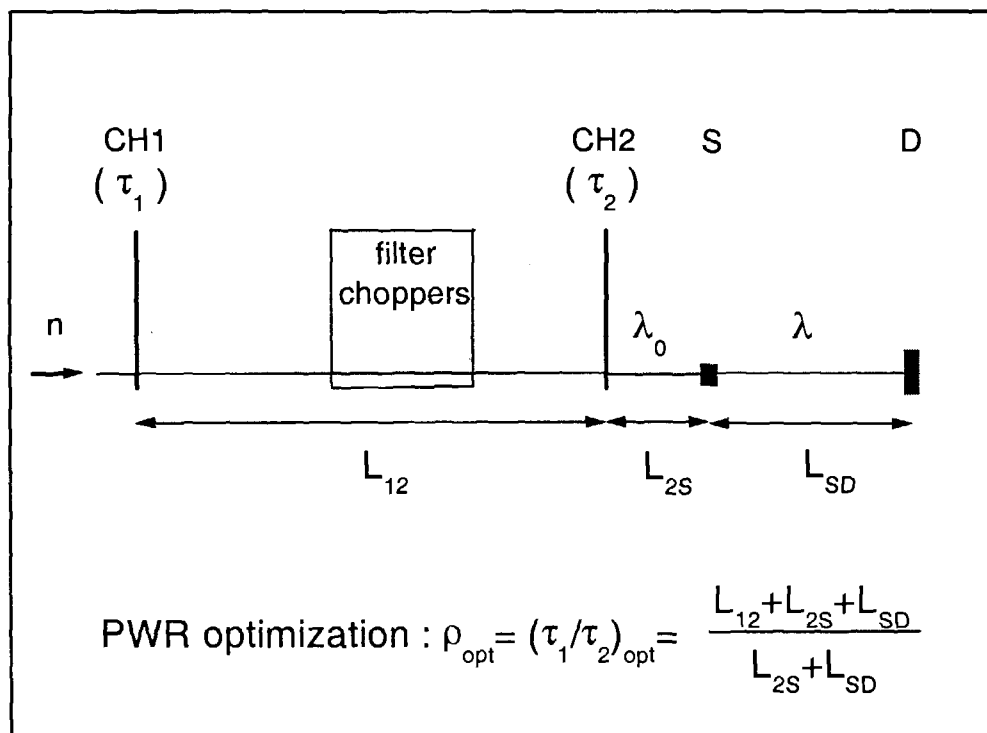


Fig. 1 Schematic sketch of a multi-disk chopper time-of-flight (MTOF) spectrometer : CH1 and CH2 are the two principal choppers defining the monochromatic neutron pulse and its wavelength bandwidth; S = sample, D = detectors; L_{12} , L_{2S} , L_{SD} are the distances between these elements of the instrument; τ_1 , τ_2 are the widths of the pulses created by CH1 and CH2, λ_0 , λ the incident and scattered neutron wavelengths. Inset : the pulse-width ratio (PWR) optimization formula for elastic scattering.

equal. This equation shows, that for any optimized spectrometer configuration the opening time of the last chopper (CH2 in Fig. 1) will have to be appreciably shorter than that of the first chopper (CH1 in Fig. 1). In order to achieve this, even in the case of highest resolution requiring highest chopper speed near the limit of mechanical resistance of the disk material, one has to resort to some means other than the speed for reducing the pulse width τ_2 . The tool invented for this purpose is a beam compressor in the form of a double-trumpet [12], which will be further discussed in Sec. 5.

Relation (4) is quite general in the following sense : It applies for all elastic and inelastic scattering experiments. It does not explicitly depend on the pulse widths, τ_1 and τ_2 , and it is independent of the flight-path uncertainty ΔL . We also note, that in the case of elastic scattering ($\lambda = \lambda_0$), the relation is simplified and becomes independent of the neutron wavelength (see inset in Fig. 1). This simplified version of the formula can be used for quasielastic scattering, where the optimization concerns a limited energy transfer region near the energy transfer origin. Since the value of ρ_{opt} is fixed, for any given energy transfer, as soon as the spectrometer dimensions have been decided (for instance, in the case of NEAT, for elastic scattering, ρ_{opt} was chosen to be close to 4), the PWR optimization relation (4) should be an indispensable tool during the concept-finding period of any MTOF spectrometer development.

In order to allow experiments to be carried out, employing a wide range of energy resolutions, it is also desirable to be able to vary the pulse widths, τ_1 and τ_2 , over ranges as large as possible. In the case of NEAT a variation of both widths over two orders of magnitude can be achieved for any given incident neutron wavelength by changing the chopper speed (from 750 to 20000 rpm), and / or by selecting different chopper windows, and / or by switching between single and double-chopper mode of operation. Clearly, whenever τ_1 and τ_2 are to be set for an experiment, the PWR optimization relation (4) should be applied, in order to provide the highest intensity, that can be obtained at the desired resolution.

The pulse-width ratio ρ is one of the important factors controlling the spectrometer efficiency. More generally, in order to allow also a comparison of the intensity-resolution relationships for different (e.g. non-Gaussian) pulse shapes, it may be useful to define it as $\rho = \sigma_1 / \sigma_2$, where σ_1 and σ_2 are the standard deviations of the neutron-pulse time distributions created by the first and by the last chopper (or chopper pair) of the spectrometer. This does however not change the essential results of the discussion in this and the previous Section. Which one of the possible "pulse-width" definitions is the most suitable for this purpose, depends on the type of experiment. It is well known, that the requirements regarding this question are quite different, for instance in the different cases, where the resolution is needed either to separate two sharp peaks, or to isolate a tiny quasielastic signal underneath a huge elastic component.

The number of possible ρ -values is restricted, because chopper speed ratios have to be integers and because only a finite number of different slots can be accommodated on a chopper disk. Obviously for each experiment the ρ -value selected should be close to the optimum number ρ_{opt} corresponding to the highest possible intensity for a given energy resolution. Intensity optimization calculations for the spectrometer NEAT have shown [11], that such a ρ -value can always be found for any resolution in the available $\Delta(hv)$ - range. In Fig. 2 an example of such a calculation is presented. Two spectrometer configurations, which give the same energy resolution ($\Delta(hv) = 103.8 \mu\text{eV}$) are shown together with their respective PWR optimization curves. The latter differ by an intensity factor of 1.6, due to the use of chopper windows (CH1, 60 mm; CH2, 30 mm) twice as wide as the guide (30 mm ; 15 mm) in one of the configurations (labeled No. 14 in the figure), which allows a higher chopper speed to be employed. At fixed resolution this leads to a resolution shape with sharper edges and therefore favorizes the integrated intensity. In addition, this configuration is optimized

(chopper speeds: CH1, 6659 rpm; CH2, 13318 rpm), with $\rho = 4$, i.e. close to the ideal value $\rho_{\text{opt}} = 4.125$ of NEAT. The second configuration (labeled No. 18 in the figure), which is not fully optimized (both chopper speeds : 6720 rpm), with $\rho = 2$, presents an intensity loss factor of 0.78, as compared to full PWR optimization using the same chopper windows.

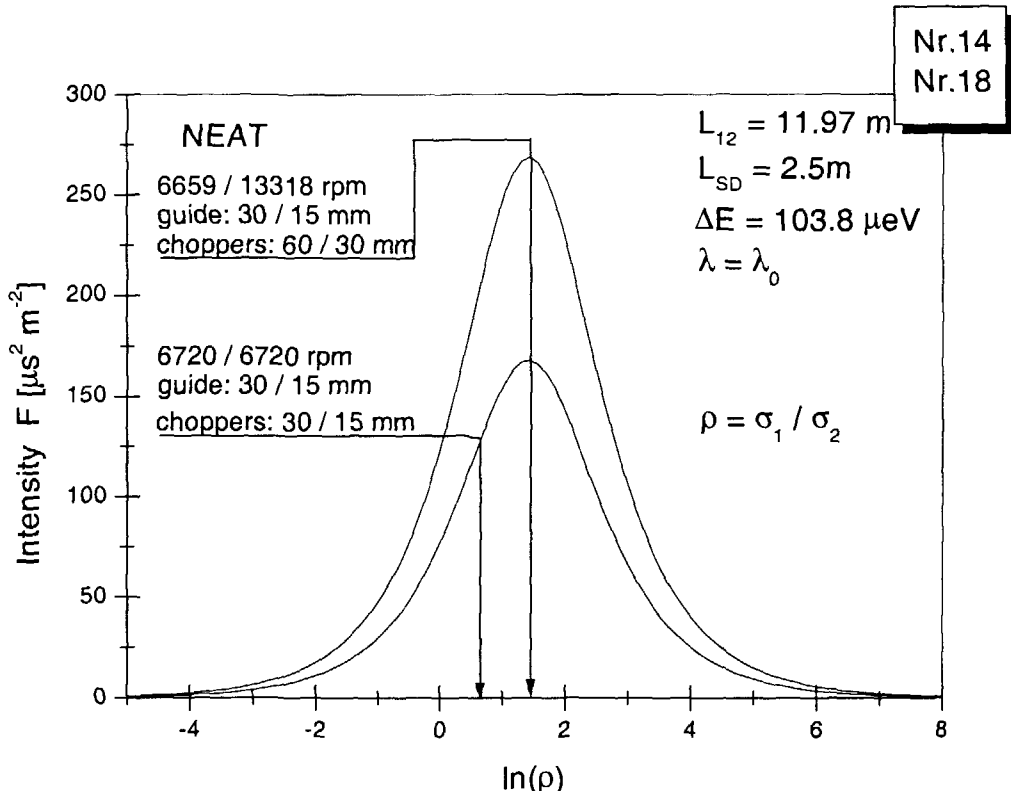


Fig. 2 Example of an intensity optimization calculation for NEAT: Two spectrometer configurations, which give the same energy resolution ($\Delta(h\nu) = 103.8 \mu\text{eV}$) are shown together with their respective PWR optimization curves. The latter differ by an intensity factor of 1.6, due to the use of chopper windows (60 / 30 mm) twice as wide as the guide (30 / 15 mm) in one of the configurations (labeled No. 14 in the figure), which allows a higher chopper speed to be employed. At fixed resolution this leads to a resolution shape with sharper edges and therefore favorizes the integrated intensity; see text for more details.

4. PWR optimization at a pulsed source

The relations concerning intensity, resolution and optimum PWR, derived for MTOF spectrometers at continuous sources, which were given in Sections 2 and 3, respectively, are essentially also valid at pulsed sources. The time-structure of the pulsed source flux however results in certain restrictions regarding the values of relevant parameters, which will have some consequences concerning the details of the optimization procedure. This will be discussed in the following by considering the various factors determining the total intensity according to eq. (1).

The incident flux $\Phi(\lambda_0)$ is here no longer constant. The source pulse rises within a relatively short time, of the order of 10 to 20 μs , to the peak flux value and then decays much more slowly, depending on the choice of the moderator and on the neutron wavelength under consideration. Because of its long tail, the source pulse should in general not be used directly, but taylored instead, using a chopper placed as close as possible to the moderator. Fortunately we do not have to invent a new device, because naturally this task can be taken over by CH1 (see Fig. 1) of the MTOF spectrometer. Nevertheless, after having cut off the tail, the pulse created will generally not be completely symmetric. Although this will have to be taken into account with precision in the later analysis of measured spectra, it does not have a large effect concerning the present purpose, i.e. we can continue to base the discussion on eqs. (1) to (4), using the FWHM (τ_1, τ_2) of the chopper pulse time distributions, or – in the case of rather asymmetric pulses – the standard deviations (σ_1, σ_2) of these pulses instead. There are however two real restrictions, which are connected with the time structure of the source [9]. The first concerns the fact, that the opening time of CH1 should not – or more generally : the width of the pulse leaving CH1 can not – be larger than the (wavelength-dependent) duration of the source pulse, as transmitted from the moderator to CH1:

$$\tau_1 \leq \tau_s(\lambda_0) \quad (5)$$

where $\tau_s(\lambda_0)$ is the FWHM of the source pulse for the wavelength λ_0 to be selected by the MTOF spectrometer. For wavelengths in the range of 4 Å to 10 Å, where τ_s is expected to be of the order of 100 μs to 200 μs (and for even longer wavelengths), this would leave room for the variation of τ_1 down to the minimum that is feasible (e.g. in the case of NEAT choppers : 15 μs). For shorter wavelengths (e.g., $\tau_s \approx 20 \mu\text{s}$ to 30 μs) we are close to the shortest pulse width, that can be obtained with present disk-chopper technology for a reasonable guide width, and therefore not much variation of τ_1 is possible in this case. This may be considered as a challenge concerning the development of better choppers. In the mean-time the variation of intensity and resolution – in this limiting case – is restricted to what can be achieved by changing τ_2 and in certain cases (see below) the sample-detector distance L_{SD} (see eq. (3)). The question is now, how the spectrometer should be optimized under these conditions. The answer depends on the priorities regarding experiments to be carried out. Let us consider a few different cases (see also Table 1).

Case 1 (this is in fact the example considered in [1]): Suppose we give priority to highest intensity at highest resolution, when using the maximum value of $\tau_1 = 200 \mu\text{s}$ at the comparatively long wavelength of $\lambda_0 = 10 \text{ \AA}$, as well as a smallest possible opening time $\tau_2 = 15 \mu\text{s}$. Using the values, $L_{2S} = 1.5 \text{ m}$ and $L_{SD} = 2.5 \text{ m}$, which are reasonable, especially for the traditional field of large-angle scattering experiments, eq. (4) applied to elastic scattering gives $L_{12} = 49.333 \text{ m}$ and the elastic resolution (from eq. (3)) is $\Delta(hv) = 11.1 \mu\text{eV}$, which is very close to what is obtained with NEAT using $\lambda_0 = 10 \text{ \AA}$ at the highest possible chopper speed (20000 rpm). The corresponding intensity factor (see Sec. 2) is $F_i = 60.8$. Since this configuration is already optimized, one can not improve the resolution much by reducing τ_1 : For $\tau_1 = 15 \mu\text{s}$, we would have the only slightly smaller value, $\Delta(hv) = 10.3 \mu\text{eV}$, but by this measure the intensity for the same wavelength would decrease by a factor 13.3. Note however, that this loss factor does not apply, if τ_1 is decreased at shorter λ_0 – values down to the source pulse width which is shorter at smaller wavelengths, because in that case we continue to make full use of the pulse. The next question is, how the resolution width can be increased: this is achieved by increasing τ_2 . With the chopper design of NEAT the maximum value obtainable would be $\tau_2 = 1500 \mu\text{s}$, which would yield an upper limit for the resolution width of $\Delta(hv) = 420 \mu\text{eV}$, slightly smaller than that of NEAT for this wavelength (570 μeV).

At the same time the intensity would increase by a factor 100, as compared to the example with $\tau_2 = 15 \mu\text{s}$. Consequently it can be said, that this MTOF spectrometer model has a similar resolution performance as NEAT, but - because of the restriction which governs τ_1 - in the slightly more limited range, $11 \mu\text{eV} \leq \Delta(\text{hv}) \leq 420 \mu\text{eV}$. The total intensity of this spectrometer (even without modifying its basic components, except for the distance L_{12}), when placed at ISIS or at one of the projected new spallation sources (SNS, JSNS, ESS, AUSTRON, ...) would however be very much higher than those of the instruments of this type presently existing at steady-state reactor sources [1] (see also Sec. 6).

Case 2 : Let us now optimize a configuration for the shorter pulse width, $\tau_1 = 60 \mu\text{s}$, while keeping $\tau_2 = 15 \mu\text{s}$, as well as $L_{2S} = 1.5 \text{ m}$ and $L_{SD} = 2.5 \text{ m}$. This corresponds to $\rho_{opt} = 4$, leads to the chopper distance value $L_{12} = 12 \text{ m}$, and is very close to the design of NEAT; for $\lambda_0 = 10 \text{ \AA}$ one obtains $\Delta(\text{hv}) = 11.9 \mu\text{eV}$ and $F_i = 75$.

Case 3 : A configuration with $\rho_{opt} = 2$ could have the parameters, $\tau_1 = 30 \mu\text{s}$, $\tau_2 = 15 \mu\text{s}$, $L_{2S} = 1.5 \text{ m}$, $L_{SD} = 2.5 \text{ m}$ and $L_{12} = 4 \text{ m}$. For $\lambda_0 = 10 \text{ \AA}$, this would result in $\Delta(\text{hv}) = 14.4 \mu\text{eV}$, with $F_i = 112.5$.

Case 4 : Finally, we consider a configuration, which is suitable for quasielastic small-angle scattering. This requires higher energy resolution and consequently a larger sample-detector distance than the previous examples. When L_{SD} is large, an even larger value of L_{12} is

Case	ρ_{opt}	ρ	τ_1 [μs]	τ_2 [μs]	L_{12} [m]	L_{SD} [m]	$\Delta(\text{hv})$ [μeV]	F_i	P_{spec} [μs]	P_s for 60 Hz (P_s 50 Hz)	P_s 10 Hz
										16667 [μs] (20000 [μs])	10^5 [μs]
1	13.33	13.33	200	15	49.3	2.5	11.1	60.8	9479	spectra from	
	13.33	1	15	15	49.3	2.5	10.3	4.6	9479	2 to 3 dif-	
	13.33	0.133	200	1500	49.3	2.5	420	6081	9479	ferent λ_0 - values can	
2	4	4	60	15	12	2.5	11.9	75	9479	be accom-	
3	2	2	30	15	4	2.5	14.4	112.5	9479	modated	
4	4	4	30	7.5	81	25.5	1 (0.37) for 10 \AA 3 (1.7) for 6 \AA	2.777	96688	N = 6 (N = 5)	1 to 2 λ_0 - values

Table 1. Four layout examples of optimized MTOF spectrometers. Among these, Cases 1 and 4 are suitable for a spallation source : Case 1 is a large-angle quasielastic-scattering version of a MTOF spectrometer. Cases 2 and 3 are also optimized versions for the same purpose, but in practice not feasible because of spatial restrictions near the moderator (see text). Case 4 is optimized for small-angle quasielastic scattering. The (elastic) resolution is given in column 8 for $\lambda_0 = 10 \text{ \AA}$, except for the values in the 2nd last line (Case 4). The detector thickness was assumed to be 15 mm. The resolution values in parentheses refer to 1mm thin detectors. The last two columns show information concerning the question, whether chopper frequency reduction or multichromatic operation (more than one λ_0 - value) is advisable (see Sec. 5).

advantageous. Let us assume the following optimized parameter values: $L_{12} = 81$ m, $L_{2S} = 1.5$ m and $L_{SD} = 25.5$ m, $\tau_1 = 30 \mu\text{s}$ and $\tau_2 = 7.5 \mu\text{s}$, where $\rho = \rho_{opt} = 4$. One obtains the following elastic resolutions, $\Delta(hv) = 1 \mu\text{eV}$, $(0.37 \mu\text{eV})$ for $\lambda_0 = 10 \text{ \AA}$ and $\Delta(hv) = 3 \mu\text{eV}$, $(1.7 \mu\text{eV})$ for $\lambda_0 = 6 \text{ \AA}$. The first values have been calculated for conventional ^3He -detectors (15 mm thick), the values in parentheses are given for 1 mm thin detectors, which should preferably be used at small angles, in order to remove the major source of flight-path uncertainty. In this case the resolution width can be increased by changing both pulse widths, τ_1 and τ_2 , and by reducing the sample-to-detector distance, with corresponding increases in intensity. It is seen, that this spectrometer example also presents a rather competitive performance (see Table 1).

Finally, we note at this point, that the smaller distances L_{12} obtained in the cases 2 and 3 are not feasible at the pulsed source, because CH1 has to be close to the moderator and there is not enough space to install a MTOF spectrometer with full range of scattering angles at such short distances from the source. Actually, for the same reason, the moderator-to-sample distance L_{MS} at steady-state neutron sources is of the order of 50 m, but without the restriction, that CH1 has to be close to the source : $L_{MS} = 47$ m in the case of NEAT at BENSC, 57 m in the case of MIBEMOL at LLB, 45 m in the case of IN5 at ILL. Therefore it can be said, that we will not have any additional beam transport losses due to long distances at the pulsed source, as compared to the case of the research reactors.

The second real restriction connected with the time structure of the pulsed source resides in the fact, that the time-of-flight period P of the instrument can not be shorter than the constant period P_s of the source, defined by its frequency:

$$P \geq P_s \quad (6)$$

The consequence of this inequality can be understood by looking at eq. (2), which allows to determine an optimum period for given values of L_{SD} and λ_0 . If P is restricted according to (6), we can derive optimum values of λ_0 or L_{SD} from the same equation [9]. Three cases are possible, depending on the relative size of the desired spectrum length P_{spec} as compared to the source period ; let us first consider large values of P_{spec} :

$$P_{spec} > P_s \quad \text{implies that } (\lambda_0 \text{ or } L_{SD}) > \text{optimum} \quad (7a)$$

For instance, if $L_{SD} > (L_{SD})_{opt}$, the required P - value is larger than P_s , and the frequency of the neutron pulses arriving at the sample should be reduced (in practice by an integer factor N). This leads to a corresponding loss in intensity, since the overlap of spectra from consecutive pulses must be avoided, a situation known to occur frequently in the high-frequency operation of MTOF spectrometers at continuous sources. Given the low frequencies of spallation sources ($P_s = 16667 \mu\text{s}$ at 60 Hz, $P_s = 20000 \mu\text{s}$ at 50 Hz, $P_s = 100000 \mu\text{s}$ at 10 Hz), this kind of loss is less likely to occur there; for comparison: the NEAT pulse frequency can be varied between 25 Hz and 666 Hz.

No further action is required, if

$$P_{spec} = P_s \quad \text{implying that } (\lambda_0 \text{ or } L_{SD}) \approx \text{optimum} \quad (7b)$$

Regarding small P_{spec} values, the following can be said :

$$P_{spec} < P_s \quad \text{implies that } (\lambda_0 \text{ or } L_{SD}) < \text{optimum} \quad (7c)$$

If, for instance, $L_{SD} < (L_{SD})_{opt}$, then the period P_s is longer than necessary as compared to the useful length of a time-of-flight spectrum P_{spec} . In this case, monochromatic operation would

fill only part of the period with a statistically significant intensity of the spectrum of scattered neutrons. Although, in principle, the spectrum extends to infinite time-of-flight t , it dies out before the end of the period, leaving behind a gap, because of the factor t^4 in the double-differential cross-section as a function of t . No data are lost, but this in principle represents an opportunity for intensity gain by filling the gap with one or several additional spectra due to different incident neutron wavelengths, and hence different arrival times, if the gap is sufficiently long. Such multichromatic operation of the chopper cascade (see Sec. 5.4) will obviously make the measurements more efficient.

The remaining two factors in eq. (1), relevant for the total intensity, are the guide transmission, $T_g(\lambda_0)$, and the integrated detector solid angle, $\int d\Omega$. The transmission depends on the geometry, dimensions and on the quality of the coating of the neutron guide delivering the neutrons to the sample. With a large moderator-sample distance L_{MS} , for instance caused by the requirement of a large value of L_{12} , it is rather important to carefully design this part of the instrument. This will be discussed in the next Section. The intensity is obviously also maximized by maximizing the total solid angle, under which the detectors are seen from the sample position. While, in principle, larger sample-detector distances yield higher resolution, the requirement of a large solid angle and budgetary considerations will generally lead to a compromise concerning the value of L_{SD} (see Sec. 6).

5. Tools for the realization of PWR optimization

In this Section a number of tools will be discussed, which have been invented to enhance the possibilities of realizing optimum intensity at the desired resolution, as well as the range of obtainable energy resolutions. These tools are static phase-space transforming components, arrays of such components, and multiple-bandpass filter arrangements, which are integral parts of chopper cascades.

5.1 Phase-space transformers

As shown in Sec. 3 (eq. (4)), the opening time of CH2 has to be appreciably shorter than that of CH1 for any optimized spectrometer configuration. If first and last choppers were connected by a straight neutron guide of constant width, at highest resolution (where chopper window widths should be equal to horizontal guide apertures) both opening times, τ_1 and τ_2 , would be the same. This would not allow an optimization according to eq. (4). The best result (highest intensity) is obtained, if on the one hand the beam is transported through a large beam cross-section (large integrated flux and minimized losses due to fewer reflections from the walls of the guide), and if on the other hand the beam is narrow at the last chopper (short pulses and therefore high resolution). In the spectrometer NEAT, this has been achieved by implementing a beam compressor-decompressor or "double-trumpet" neutron guide arrangement [12]. Fig. 3 shows it schematically : A sequence of neutron guide sections, consisting of a conventional ^{58}Ni -coated straight guide section (SGS), with parallel walls, followed by a converging guide section (CGS) just before the last chopper of the cascade, and a diverging guide section (DGS) just after this chopper. The latter two guide sections are supermirror (SM)-coated, in order to compensate for the inclination of the double-trumpet side-walls and thus to minimize transmission losses. The double-trumpet is characterized by the real-space reduction (or beam-compression) factor $\beta = B/b$ (B = width of the parallel-walled guide, b = width at the end of the CGS, and at the beginning of the DGS), and by the divergence quotient $M = m_t / m_s$ ($m_t = \gamma_{SM} / \gamma_{^{58}\text{Ni}}^{\text{nat}}$ = ratio of the SM limiting reflection angle over that of a guide with ^{58}Ni coating; this ratio is equal to 2.4 in the case of NEAT; $m_s = \gamma_{^{58}\text{Ni}} / \gamma_{^{58}\text{Ni}}^{\text{nat}}$ = ratio of the straight guide's critical reflection angle over that of a guide with

^{nat}Ni coating; this is equal to 1.2 in the case of NEAT). Note, that the largest beam-compression without appreciable transmission losses in the double-trumpet is obtained for $\beta = M$. The wavelength-dependent oscillatory behaviour of the transmission has been theoretically predicted [13] and confirmed by Monte-Carlo calculations [14]. A value of 2 has been chosen for the beam-compression factor, because at the time of construction of NEAT the practically obtainable limit of m_t was 2.4. The reduction of the beam-width by a factor 2 at the position of CH2 results in a reduction of τ_2 by the same factor, if the chopper window width and neutron guide aperture at this location are chosen to be the same. Obviously larger reduction factors will be achieved by increasing m_t , when the SM coating technology permits it.

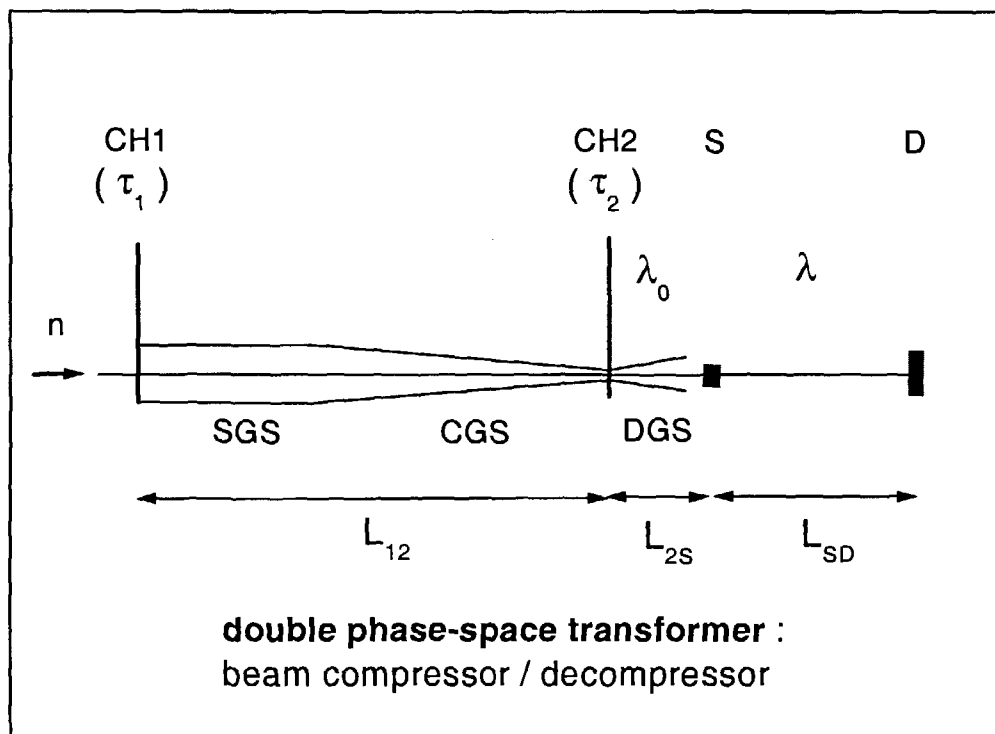


Fig. 3 Schematic view of a double-trumpet consisting of a pair of converging (CGS) and diverging (DGS) neutron guide sections with the purpose of compressing the pulsed beam in space and time at the chopper disk CH2, and subsequently decompressing it, in order to reduce the divergence of the beam at the sample. SGS = straight (parallel-walled) guide section.

The double-trumpet is a static double phase-space transformer trading beam-width against divergence using a CGS just before CH2, and vice versa trading divergence against beam-width using a DGS just after CH2. The first spatial transformation step results in a compression of the neutron pulse in time, which allows the desired improvement in resolution and an extension of the available regime for PWR-optimization (see Sec. 3) to be obtained. The second transformation step corresponds to a decompression of the beam. It spatially reverses the first step, while it obviously has no effect on the time compression. This second

step is required, in order to "refocus" the beam onto the sample by reducing its divergence and thus giving it more of a "forward direction". This, and the use of the appropriate parameter values ($\beta = M$) ensure a high transmission of the device, which in the case of NEAT varies from about 0.94 to 0.82, when λ_0 increases from 2.5 Å to 10 Å.

5.2 Pairs of double-trumpets

It is a piece of common wisdom that the beam transport over large distances between the choppers (see Sec. 4) must benefit from the largest possible neutron guide cross-section, in order to minimize the number of reflections and thus the losses connected with them. Already in the past, guide cross-sections have been maximized; but with the advent of supermirror coatings with larger m -values (up to $m = 4$) than previously available, a further increase has become possible. Such a large and long guide has been called "ballistic" [15], but we should not be misled: even with the largest guide cross-sections conceivable today, less than 10 % o

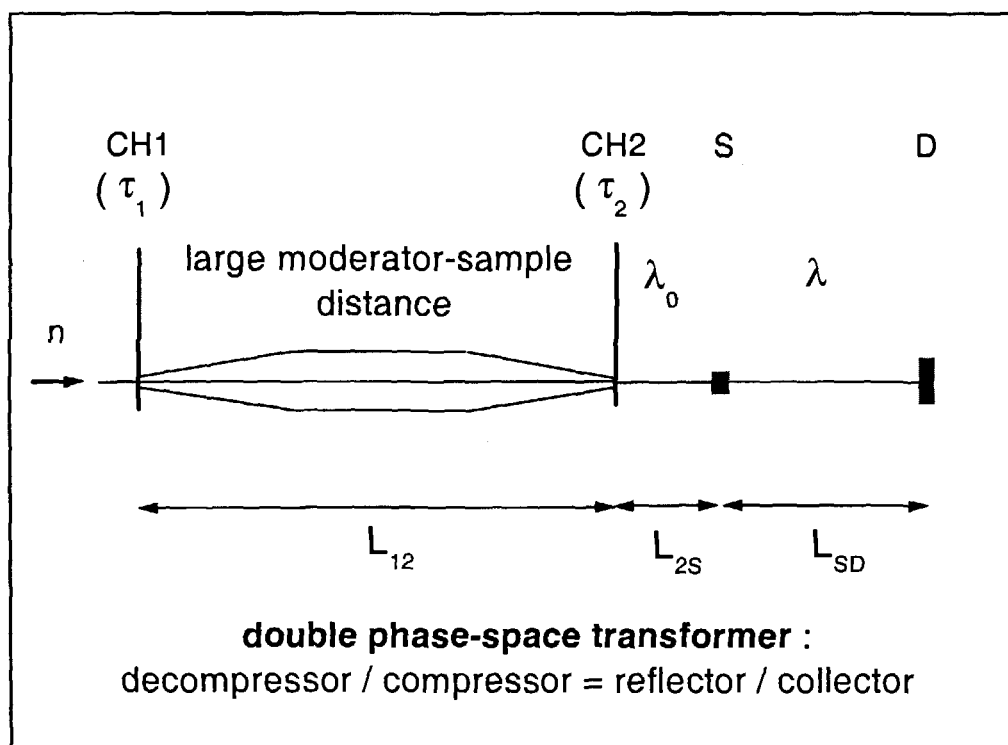


Fig. 4 Schema of a double phase-space transformer starting with a beam decompressor for the purpose of minimizing transmission losses upon beam transport over a large distance, and ending with a compressor for focussing the beam at the second chopper.

Of (e.g.) 6 Å neutrons are involved in a truly ballistic flight, if the distance is of the order of 50 m. For very large beam cross-sections to be obtained for the transport over the long distance, it is however probably necessary to decompress the beam over a certain distance beginning near the moderator, if - due to spatial restrictions or for optimization purposes - it

has to be narrow at the start, or just after CH1 (see Fig. 4), respectively. At the end, i.e. just before the last chopper the beam is compressed again for the purpose described in Sec. 5.1. In fact, in the context of applications in MTOF spectrometers this picture is incomplete, because – as we have seen above – the use of a double-trumpet at CH2 should be beneficial enough to make this recommendable. Furthermore, in future instruments of this type, it may be of interest to implement a double-trumpet not only at CH2, but also at CH1 (see Fig. 5), even if the beam should be compressed to a lesser extent at the latter. Since the pulse width is controlled by the width of the chopper window and by the horizontal guide aperture, such a device at CH1 can be used to obtain shorter rise and decay times of the pulse for a given pulse width – which leads to an effective improvement of the energy resolution without sacrificing intensity. The feasibility again depends on the space available close to the moderator and on the extent of competition from other beam lines for this space.

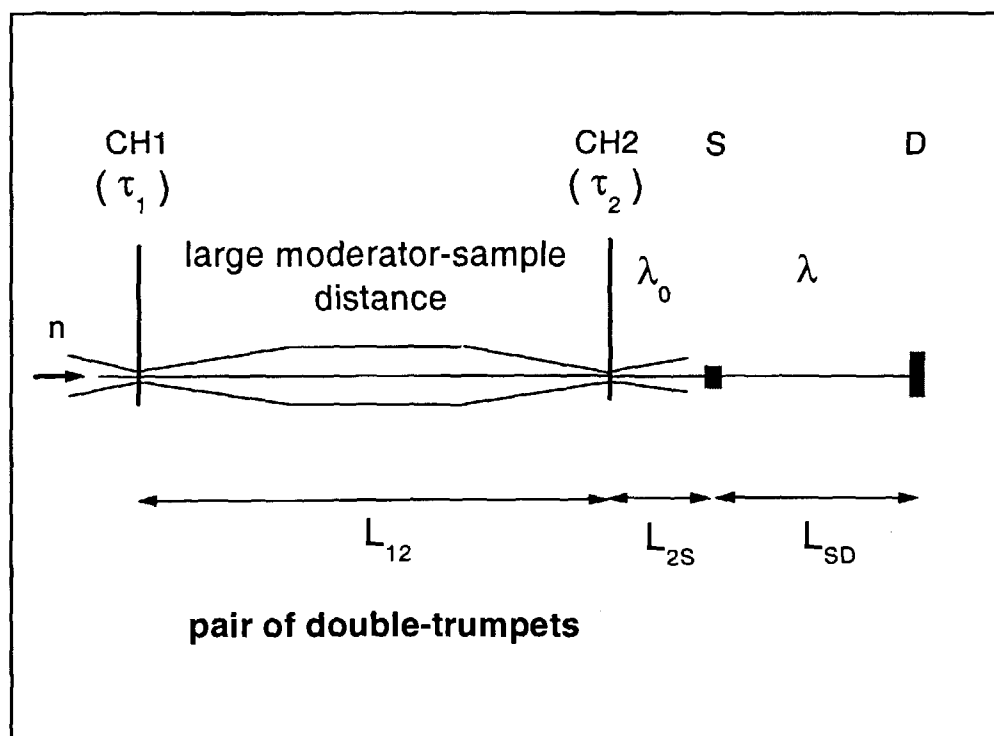


Fig. 5 Schematic sketch of a pair of double-trumpets implemented at the two principal choppers for intensity-resolution optimization; see discussion in the text.

5.3 Band-pass filters

The chopper cascade of a MTOF spectrometer is a neutron wavelength band-pass filter. A simple pair of disk choppers yields a multichromatic pulsed neutron beam containing a series of discrete bands of different neutron wavelengths, as soon as the distance L_{12} is larger than a certain limit $(L_{12})_{\text{lim}}$. For choppers with one or several windows equidistant in angle, this limit is simply proportional to the period P defined by the disk-chopper and inversely proportional to the range of wavelengths $\Delta\lambda_0$ available in the incident neutron spectrum:

$$(L_{12})_{\text{lim}} [\text{m}] = P[\mu\text{s}] / (252.78 \cdot \Delta\lambda_0 [\text{\AA}]) \quad (8)$$

For instance, if the λ_0 -range is 30 Å, and if the period is 6000 μs, this limit is about 0.8 m. Therefore, in the conventional use of such cascades (at steady-state reactor sources) employing much larger distances, the basic chopper pair, CH1 and CH2, is complemented by additional filter choppers set up in between, which have for instance the purpose of eliminating all pulses, that do not have the desired wavelength λ_0 . By this effect the chopper cascade becomes a pulsed time-of-flight monochromator. This is well-known and has been realized in the existing spectrometers [3], [5], [6], [7], [11]. To illustrate it, Fig.6 shows a neutron flight-path diagram as a function of neutron flight-time, demonstrating for the case of IN5 the way this filter technique is applied. This example corresponds to a configuration used in 1975 in a study of the rotational motion of OH ions in cubic NaOH [16], with an incident neutron wave length $\lambda_0 = 4 \text{ \AA}$. In this diagram, CH1 is located at the flight path origin and the

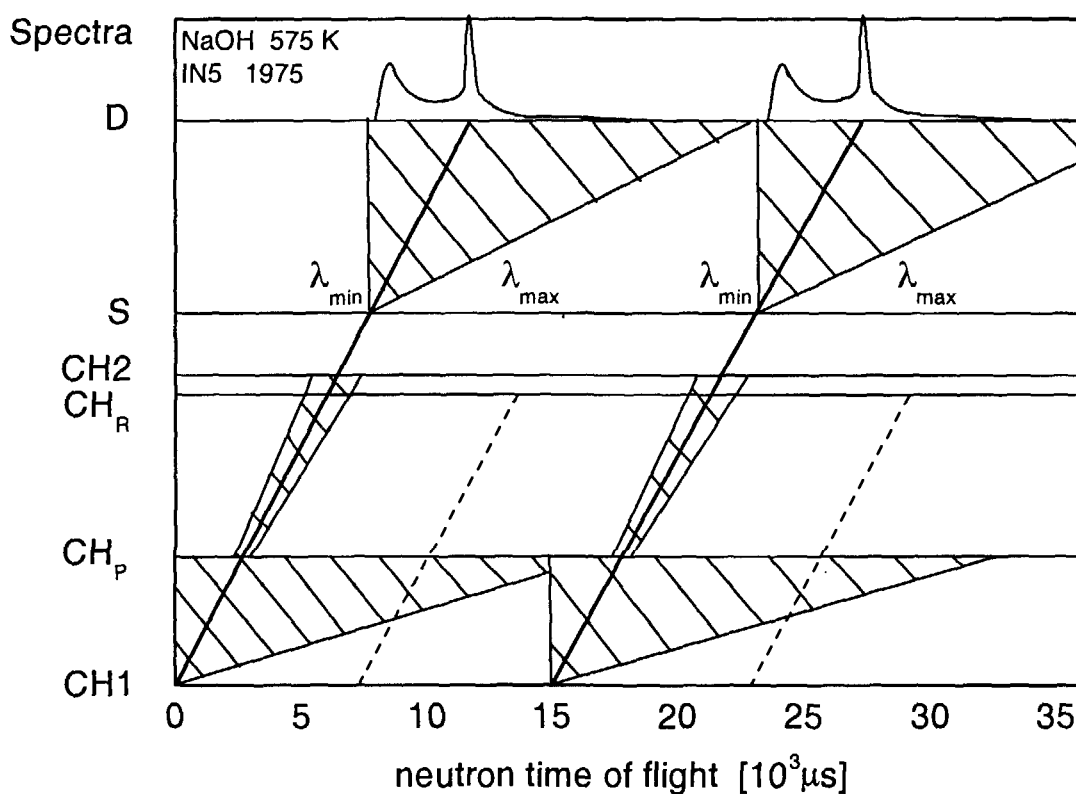


Fig. 6 Neutron flight-path diagram based on a sketch corresponding to an experiment carried out in 1975 [16] with the MTOF spectrometer IN5 at ILL, using 4 Å neutrons. It demonstrates the filter action of the various disks of the chopper cascade. The vertical axis represents the flight-path between the different elements of the chopper cascade (CH1 defines the initial time-distribution of the neutron pulse; CH_P is the pre-monochromator; CH_R is employed for pulse frequency reduction, in order to avoid frame-overlap at the detectors; and CH2 selects the 'monochromatic' wavelength band for the experiment). See text for more details.

pulsed beam is monochromatized by CH2, which opens when the required (flight-) time has elapsed, at a distance of 6.255 m from CH1. True monochromatization is however only possible after a crude pre-monochromatization by a filter-chopper CH_p placed at a distance of 2.6 m from CH1, which stops the larger part of the "white" spectrum (hatched areas between the horizontal lines representing the positions of chopper disks CH1 and CH_p in Fig. 6). This prevents the occurrence of "different order" pulses, i.e. the passage of pulses with different flight times (different slopes in the flight-path diagram, i.e. different neutron velocities) and therefore wavelengths different from the desired one. The inclined heavy solid lines indicate the flight of neutrons with the selected wavelength λ_0 , which are the only ones allowed to cross the (horizontal) position line of CH2 in this diagram.

In order to avoid frame-overlap at the detector, i.e. superposition of spectra originating from the scattering of consecutive neutron pulses by the sample, still another filter-chopper is required. In our example, this is the reduction chopper CH_R, which transmits only every Nth pulse created by CH1 at a distance of 5.851 m from the latter. Here N=2, i.e. the pulse frequency is divided by 2, whereby the period is multiplied by the same factor. The neutron pulses stopped by CH_R are shown as dashed lines. The spectra created by the remaining pulses are accumulated until sufficient statistical accuracy is obtained.

If the chopper distance L₁₂ is shorter than $(L_{12})_{\text{limit}}$, then a single pulsed wavelength band is created. The bandwidth Δλ depends on L₁₂ and on the opening times of the chopper windows. For instance, in the simple case where $\tau_1 = \tau_2 = \tau$, and if the widths of the chopper windows are equal to the guide aperture, the bandwidth (FWHM) is given by

$$\Delta\lambda [\text{\AA}] = \tau [\mu\text{s}] / (252.78 \cdot L_{12}[\text{m}]) \quad (9)$$

The bandwidth can be varied by changing the chopper speed and /or the distance. If the bandwidth is made large (pulsed "white" beam), time-of-flight diffraction experiments can be carried out (see refs. [17] to [21]). For instance, if in the spectrometer NEAT only the last pair of counter-rotating choppers is used ($L_{12} = 0.052$ m in this case), the bandwidth Δλ can theoretically be varied from as small as 1.14 Å up to as large as 60.86 Å (the practical limit being about 40 Å because of negligible incident flux at larger wavelengths). Obviously, other chopper pairs may be employed instead, and the choice is governed by the Q-resolution required in the diffraction study. After having pointed out this use of parts of the chopper cascade, we will not go into further details of this type of experiment, but briefly consider the problem of achieving the filter action of the chopper cascade as a whole in the next Section.

5.4 TOF-monochromators and multichromatic operation

Designing a multi-disk chopper cascade which acts as a time-of-flight monochromator, requires to find a configuration, i.e. a set of chopper distances together with a chopper window arrangement on each disk (specified by window widths and phase angles of the windows on each disk) ensuring the transmission of a periodic sequence of neutron pulses centered at the desired wavelength λ_0 , without contamination by other wavelengths, and with the desired time-of-flight period P. This means, that all unwanted ("parasitic" or "different-order") neutron pulses must be eliminated, that contain neutrons, which have taken an integral number of periods P less or more time than the neutrons with wavelength λ_0 to travel over the monochromator distance L₁₂. The elimination from the neutron pulse series mentioned at the beginning of Sec. 5.3 is achieved by the filtering action of intermediate chopper disks placed between the two basic choppers CH1 and CH2. It must be effective in the whole volume of the multi-dimensional configuration space to be accessible to the operation of the instrument,

i.e. for the complete ranges of incident wavelength, principal-chopper speed, sample-detector distance (if this is a variable), and for all sets of chopper windows, window widths, window-phase angles, that are available. A semi-analytical method has been used [22] to solve this problem. It consists in a systematic analytic calculation of all the neutron pulses transmitted by the chopper system, for a series of chopper system configurations. The result is represented as an ensemble of closely spaced points in configuration space. Points corresponding to pulses of the unwanted kind are rejected, whereby holes of forbidden space are created. Compact regions, which are free of such holes can be used for the design of the spectrometer. The search for these compact regions is facilitated using products of Boolean transmission functions of pairs of choppers [23] [24].

In situations of the kind described by eq. (7c), i.e. when monochromatic operation would not fill the whole period with a useful spectrum of scattered neutrons (see Sec. 4), the measurements can be made more efficient by filling this gap with spectra due to scattering of additional pulses with different neutron velocities (which then must no longer be considered as "parasitic"). Fig. 7 shows schematically, how a finite number of incident neutron wavelength bands centered at the values $(\lambda_0)_n$ is used for this purpose. This procedure, which

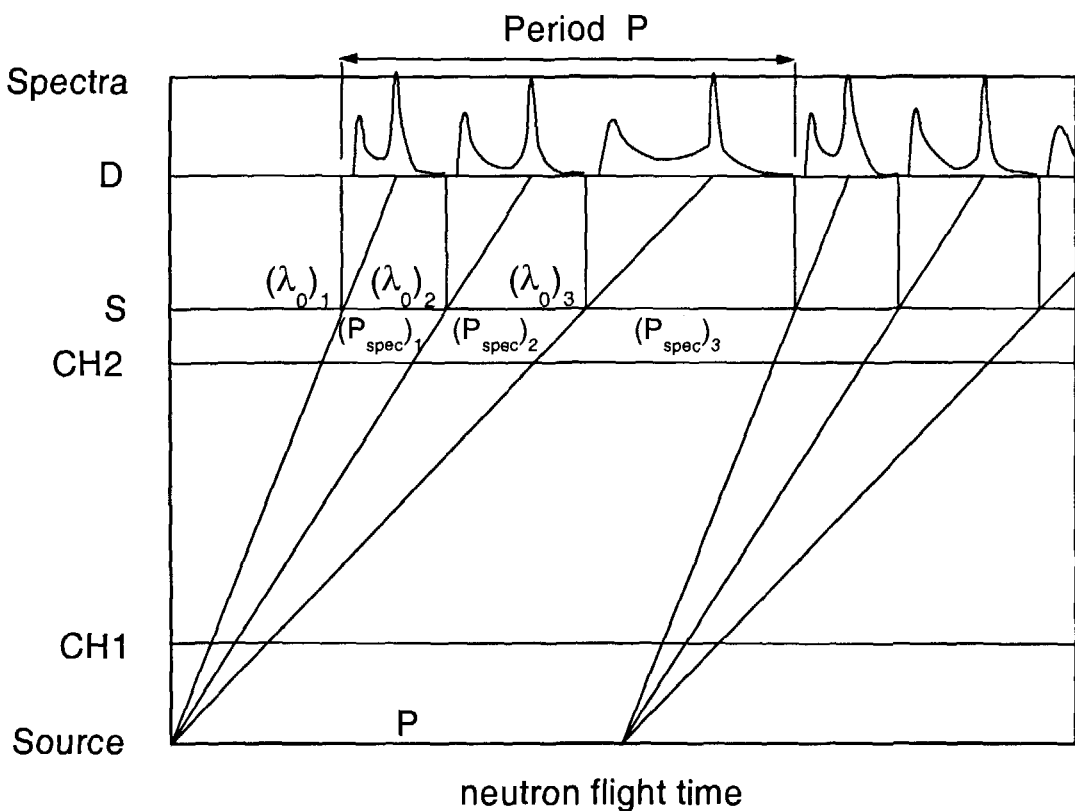


Fig. 7 Schematic diagram of multichromatic operation of a MTOF spectrometer. Three different incident neutron wavelengths are selected by the chopper cascade so, that the three corresponding spectra of scattered neutrons fill consecutively the period defined by a low pulsed source frequency. The sum of the 3 spectral periods is equal to the source period P .

is an inherent possibility of properly designed MTOF spectrometers, has been called "repetition rate multiplication" [25] referring to the fact that the repetition rate of the spallation source is too low for an efficient use of the incident flux in the considered situation. A more appropriate name for this method is "multichromatic operation", since the repetition rate is neither modified by this procedure, nor is the effectively useful period P resulting from it an integer multiple of the spectral period P_{spec} that would be used in monochromatic operation in the otherwise identical spectrometer configuration. The practical implementation of multichromatic operation modes, in principle, requires the same kind of calculations as described above for monochromatic operation, with an appropriate definition of the corresponding compact regions in configuration space.

6. Solid angle and total spectrometer intensity

A new MTOF spectrometer should of course be optimized with respect to each of the factors in the intensity equation (1). At any one of the new spallation source projects, it will have a much higher intensity at given energy resolution than any existing instrument of the same type because of i) source-related and ii) instrument-specific improvements.

i) *Source-related gain factors* : The MTOF-spectrometer principle is intrinsically adapted to pulsed sources, because it employs a pulsed mode of operation itself. If we assume a peak flux of 1×10^{16} neutrons $\text{cm}^{-2} \text{s}^{-1}$, for instance at the AUSTRON source, and compare to the same instrument at the BER-II medium-flux reactor (where NEAT is located), the flux gain factor for AUSTRON is as much as 80. In other words: the intensity of NEAT would be increased by a factor of 80, if this instrument was moved without drastic modifications to the AUSTRON source. For a more conservative estimate of the possible gain, we will retain a factor of 40 (instead of 80) at this point.

ii) *Instrument-improvement gain factors* : Starting from the present design of NEAT, a number of modifications are possible, in order to increase the integral intensity at the detectors, essentially without changing the energy resolution performance of the instrument. We list only a few of these possibilities in the following. Integral intensity may be gained (see also Table 2) :

- by increasing the beam height at the entrance to the chopper system; this requires spatial focusing in the vertical plane at the sample position;

Table 2. *Intensity gain factors to be achieved by various measures of improvement*

Improvement	Comment	Gain factor	Total gain
Double the beam height	55 mm → 110 mm + vertical focusing	1.6	1.6
SM guide includ. beam compressor	gain factor: 4 loss factor: 2	2	3.2
max. solid angle $90^\circ \times 137^\circ \times 2$ L2S = 1.33 m	use of conventional SDs with solid angle gaps	4.6	14.7
max. solid angle $90^\circ \times 170^\circ \times 2$ L2S = 3.33 m	benefit of larger Q - range	1.24	18.2
use of piggy-pack SDs or PSD	with negligible solid angle gaps	2.65	48

- by using supermirror (SM) coated neutron guides with larger m-values, for instance $m = 2$ in the straight guide and $m = 4$ in the double trumpet;
- by increasing the solid angle (of scattering) covered with standard ^3He single detectors (SD): in the horizontal plane both positive and negative scattering angles may be used; vertical scattering angles may be extended up to $\pm 45^\circ$ (rather than $\pm 20^\circ$ available now); this requires a modification of standard sample-environment equipment, such as cryostats, furnaces, etc., which is feasible without difficulty;
- by increasing the Q-range in the horizontal plane, when removing the spatial restriction caused by the condition, that the chopper-sample distance L_{2s} be minimized; this is an acceptable compromise, since the length of the TOF-monochromator L_{12} has to be increased to about 50 m for the instrument at the spallation source;
- by removing large solid angle gaps between the detectors, that exist in present-day instruments; this requires replacing the standard ^3He single detectors by a close-packed detector system (for instance obtained by tessellation of scintillation detectors carrying photomultipliers and electronics in a piggy-back arrangement); it might also consist of a large position-sensitive detector (PSD) assembly, however not necessarily with the requirement of very high spatial resolution;

The numerical example given in Table 2 shows, that all in all the integral intensity, i.e. the instrument efficiency at given resolution, may be increased as compared to NEAT in its present state, by almost two orders of magnitude, if the listed elements of improvement are fully exploited. For a conservative estimate we will however retain here a gain factor of only 25 (instead of 48).

The following (conservative) intensity gain factors, as compared to the existing MTOF spectrometer at BENSC, are thus achieved :

1.) due to the full use of the peak flux of the source (example: AUSTRON):	factor 40
2.) due to improvements of the spectrometer design:	factor 25
3.) Total intensity gain (at constant resolution):	factor 1000

Combining the conservative gain factor versions of i) and ii), we finally obtain a conservative total possible gain factor of 1000 for the new MTOF-instrument, if located at AUSTRON.

7. Conclusion

For a MTOF spectrometer placed at a spallation source, the essential difference as compared to such instruments at reactors, regarding the above-described optimization, may come from the fact, that one would like to benefit from the largest possible fraction of the peak flux of the source. This implies using essentially the source's own pulse width, which - for given wavelength and target design - is fixed. As a result of this restriction, and if we assume fixed chopper-chopper-sample-detector distances, I propose to carry out the pulse-width ratio (PWR) optimization for the highest resolution to be achieved by the spectrometer using this fixed width at a relatively large neutron wavelength (of the order of 10 Å). The compromise of non-perfect optimization, which is then to be made for lower resolutions, on the other hand, can be accepted in view of the fact, that the intensity is rapidly increasing with decreasing resolution. As a result of these considerations we obtain the requirement of a L_{12} - value (distance between first and last chopper (pairs)) of the order of 50 m, in order to obtain a resolution range comparable to that of existing MTOF spectrometers at research reactors. No additional transmission losses will arise however, because moderator-sample distances L_{MS} at

the latter sources traditionally have always been of the same order of magnitude due to space requirements.

The discussion of possible intensity gains has given rather promising results. Combining the conservative gain factors listed in Sec. 6, we obtain a conservative total possible gain factor of 1000 for the new MTOF-instrument, if located at AUSTRON, as compared to NEAT as presently operating at HMI. Obviously the gain would be even larger at the more powerful spallation sources under construction, SNS (USA), or in the planning stage, JSNS (Japan) and ESS (Europe). It should be noted, that such gain factors will increase the yield of the so far intrinsically low-intensity ‘differential type’ quasielastic and low-energy inelastic scattering studies up to the level available in present-day ‘integral type’ investigations, such as small-angle scattering and other intrinsically-high-intensity diffraction experiments. This will permit those large-scale studies to be carried out, which are urgently needed to make decisive progress in the fields of complex systems, and especially in those of the biological sciences and of biotechnology.

Finally it is worthwhile to mention, that the scientific success experienced by numerous users, when carrying out experiments with IN5, MIBEMOL and NEAT at the respective steady-state sources, has recently prompted the initiation of four new MTOF spectrometer projects, three at research reactors, namely one at NIST [26] (now being commissioned), an improvement-reconstruction project at ILL to replace IN5 [27], an instrument at the new research reactor FRM-II and one new instrument of this type at the LANL spallation source [28]. A further instrument has been proposed [1],[2]; other proposals will surely follow.

References

- [1] R. E. Lechner, *Physica B* **276-278** (2000) 67.
- [2] R. E. Lechner, in: *AUSTRON Projektstudie*, Teil 2 (Vienna 1998) 32.
- [3] R. E. Lechner, F. Douchin and R. Scherm (1973) unpublished.
- [4] R. Scherm, JüL-295-NP, Internal Report, KFA Jülich (1965).
- [5] F. Douchin, R. E. Lechner and Y. Blanc, Internal Technical Report, ITR **26/73**, ILL Grenoble (1973).
- [6] S. Hautecler, E. Legrand, L. Vansteelandt, P. d'Hooghe, G. Rooms, A. Seeger, W. Schalt and G. Gobert, in: *Neutron Scattering in the 'Nineties* (IAEA Vienna, 1985) p. 211.
- [7] R. E. Lechner, *Neutron News* **7**, No. 4 (1996) 9.
- [8] R. E. Lechner, R. Melzer and J. Fitter, *Physica B* **226** (1996) 86.
- [9] R. E. Lechner, in: *Proceedings of the Workshop on Neutron Scattering Instrumentation for SNQ*, Maria Laach 1984, Internal Report JüL-1954, eds. R. Scherm, H. Stiller (KFA-Jülich, October 1984) pp.202-220.
- [10] R. E. Lechner, in: *Neutron Scattering in the 'Nineties* (IAEA Vienna, 1985)pp.401-407.
- [11] R. E. Lechner, in: *Proceedings of ICANS-XI*, KEK Report 90-25, eds. M. Misawa, M. Furusaka, H. Ikeda, N. Watanabe (Natl. Lab. for High Energy Physics, Tsukuba, March 1991) pp. 717-732.
- [12] R. E. Lechner, in: *Advanced Neutron Sources*, Proceedings of ICANS-X, ed. D. K. Hyer (Inst. of Physics, Bristol 1989) pp.843-848.
- [13] I. S. Anderson, in: *Thin Film Neutron Optical Devices*, Proc. SPIE 983 (1988).
- [14] R. E. Lechner and F. Mezei, in: *Proceedings of ICANS-XI*, KEK Report 90-25, eds. M. Misawa, M. Furusaka, H. Ikeda, N. Watanabe (Natl. Lab. for High Energy Physics, Tsukuba, March 1991) pp. 919-929.
- [15] F. Mezei, *J. Neutron Research* **6** (1997) 3-32.
- [16] J. G. Smit, H. Dachs and R. E. Lechner, *Solid State Commun.* **29** (1979) 219-223.

- [17] R. D. Lowde, *Acta Crystallogr.* **9** (1956) 151.
- [18] B. Buras, J. Leciejewicz, W. Nitc, I. Sosnowska, J. Sosnowski and F. Shapiro, *Nukleonika* **7-8** (1964) 523.
- [19] R. M. Ibberson, W. I. F. David and K. S. Knight, Report RAL-92-31, Rutherford Appleton Laboratory, Chilton, England (1992).
- [20] B. Rufflé, J. Ollivier, S. Longeville and R. E. Lechner, *Physica B* **276-278** (2000) 170-171.
- [21] B. Rufflé, J. Ollivier, S. Longeville and R. E. Lechner, *Nucl. Instr. and Methods A* **449** (2000) 322-330.
- [22] R. E. Lechner, *Physica B* **180 & 181** (1992) 973-977.
- [23] J. R. D. Copley, *Physica B* **180 & 181** (1992) 914-916.
- [24] H. Schober, Ch. Losert, F. Mezei and J. C. Cook, *J. Neutron Research* **8** (2000) 175-185.
- [25] F. Mezei, in: *Proceedings of ICANS-XIII*, (Paul Scherrer Institut, Villigen, 1995) 400-415.
- [26] J. R. D. Copley, *Nucl. Instr. and Methods A* **291** (1990) 519-532.
- [27] H. Schober, A. J. Dianoux, J. C. Cook and F. Mezei, *Physica B* **276-278** (2000) 164-165.
- [28] F. Mezei, M. Russina and S. Schorr, *Physica B* **276-278** (2000) 128-129.